Role of boundary conditions in the annihilation of nematic point defects

G. Guidone Peroli and E. G. Virga
Istituto Nazionale di Fisica della Materia, Dipartimento di Matematica, Università di Pavia, via Ferrata 1, 27100 Pavia, Italy
(Received 11 August 1998)

We describe the effect of boundary conditions on the motion of point defects in a nematic liquid crystal confined within a capillary tube. In particular, we show how even a small tilt of the director on the lateral boundary could considerably affect the dynamics of defects. In our model the hydrodynamic flow induced by the director rotation, often called the *backflow*, is systematically neglected. We also suggest describing the backflow by introducing phenomenologically an effective rotational viscosity depending on the distance between the defects [S1063-651X(99)07102-0]

PACS number(s): 61.30.Jf

I. INTRODUCTION

In the classical continuum theory for nematic liquid crystals, which presumes the same degree of order to be prescribed everywhere, point defects are mathematically modeled as points of discontinuity for the director field

$$\mathbf{n}:\mathcal{B}\rightarrow\mathbf{S}^2, \tag{1}$$

which describes the average direction of the molecules in the region $\mathcal{B}$ occupied in space by a material sample. Here $\mathbf{S}^2$ denotes the unit sphere.

A point defect can be assigned a *topological charge*, as illustrated, for example, in [1] and [2]: it roughly corresponds to the number of times the director wraps around the unit sphere when a whole region around the defect is spanned. It is a common experience to see two defects with opposite topological charges that attract each other as soon as the distance between them is sufficiently short.

The problem of modeling this dynamical process is not the easiest one. In principle, one should rely on the continuum equations for both the flow and the director motion first proposed by Ericksen and Leslie (see [3] and [4]). Their solution, however, is likely not to be found analytically when defects are present.

In [5] we proposed a different way of attacking this problem. In considering a point defect inside a capillary tube, we renounced finding the exact minimizer for the energy functional describing the elastic distortion around a prescribed point defect; rather, to mimic a singularity, we introduced a class of director fields depending on a single scalar function. Such fields are built by appropriately *joining* together the regular solutions escaped in opposite directions, found independently by Cladis and Kléman [6] and Meyer [7]. Luckily enough, within this class of director fields the elastic energy can be minimized explicitly: this leads to prototypes for both $+1$ and -1 point defects inside a capillary tube enforcing the homeotropic anchoring for $\mathbf{n}$ on the lateral boundary. These prototypes are sufficiently versatile to describe a variety of configurations with two or more defects alternating in topological charge. We did not confine our attention to statics: by resorting to an appropriate dissipation principle, we also arrived at a genuine dynamical model, where defects are considered like particles in a dynamical system (see [8] and [9] for a deterministic study and [10] for a statistical one). Thus, in [5] we succeeded in describing the coalescence of two point defects with opposite topological charges. We predicted a finite cutoff distance d_c for the interaction between two defects, which has recently been confirmed by several numerical simulations based on an independent model [11]. For homeotropic anchoring, d_c is slightly larger than the cylinder diameter.

Though this model captures the essence of a dynamical phenomenon whose detailed description has long been lacking, recent observations suggest that it should be extended to adhere better to a more complex reality. As reported in [14], there is enough experimental evidence to hold that when the distance between two defects with opposite topological charges exceeds d_c, they approach each other at a constant speed, thus revealing a constant *capillary pressure* that acts on them before they start interacting. We showed in [14] how a slight misalignment of the nematic director at the boundary of the cylinder can be responsible for such a pressure. If the anchoring fails to be homeotropic, the distance d_c also depends on the actual anchoring, which in cylindrical symmetry is completely described by the anchoring polar angle. Our model for the annihilation of two point defects needs to be extended, since in general the boundary conditions are also likely to affect their relative motion when the defects come closer than the distance d_c. Besides this distance, the interaction force itself should also depend on the anchoring angle.

Here we illustrate a model for the interaction between two defects which move along the axis of a capillary tube, on whose boundary the anchoring fails to be homeotropic. Such a failure could possibly be induced by the filling process to an extent directly related to the filling velocity. Our development parallels the one in [5] for the homeotropic anchoring. We still renounce solving the complete equations of nematodynamics: in Sec. II we introduce an appropriate class of fields which mimic again both a $+1$ and a -1 point defect, while obeying the new boundary condition. We then minimize the elastic free energy within this special class, thus obtaining analytically a family of director fields that model two point defects at every prescribed distance. In Sec. III, we compute from the elastic free energy the interaction force between the defects. In Sec. IV we arrive at the equation that governs their motion, by only accounting for the energy dis-

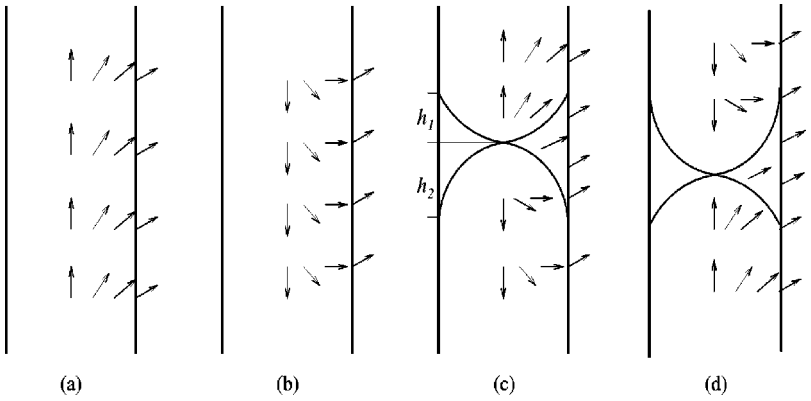

FIG. 1. (a) and (b) illustrate the fields $\mathbf{n}_-$ and $\mathbf{n}_+$, respectively; (c) and (d) illustrate a $+1$ and a -1 defect, respectively.

sipated in the rearrangment of the director field. In fact, here the hydrodynamic flow induced by the rotation of the director, often called the *backflow*, is systematically neglected. In Sec. V, we discuss this assumption. Since, as shown in both [12] and [13], the backflow can effectively be described by reducing the rotational viscosity in the director motion, we explore the consequences on the annihilation process of an effective rotational viscosity depending on the distance between the defects. We show that this indeed contributes to a finer analysis of the phenomenon.

II. MODEL FOR A POINT DEFECT

In this section we give a brief description of the extended model referred to in the Introduction: we first describe a class of fields which serve as prototypes for both $+1$ and -1 defects in the director orientation, we then find the field that minimizes the elastic free energy within this class, and we finally compute this minimum.

Hereafter we shall regard the capillary tube as a cylinder with radius R and height $2H$, and we will only consider axisymmetric fields $\mathbf{n}$ inside it, which in cylindrical coordinates (r,ϑ,z) can be written as

$$\mathbf{n}(r,\vartheta,z)=\cos\varphi(r,z)\mathbf{e}_r+\sin\varphi(r,z)\mathbf{e}_z, \tag{2}$$

where $\mathbf{e}_r$ and $\mathbf{e}_z$ are unit vectors in the coordinate frame $(\mathbf{e}_r,\mathbf{e}_\vartheta,\mathbf{e}_z)$. We assume that $\mathbf{n}$ is subject to the following boundary condition:

$$\varphi(R,z)=\varphi_0, \quad -\frac{\pi}{2}<\varphi_0<\frac{\pi}{2}, \tag{3}$$

which reduces to the *homeotropic* anchoring when $\varphi_0=0$. Here we are interested in studying the coalescence of two defects with opposite topological charges when the boundary condition fails to be homeotropic. Actually, Eq. (3) requires the angle φ to be constant along z and independent of time, a condition which is compatible with the *conical* anchoring. This is a degenerate anchoring, where only the angle between the normal to the cylinder and the nematic director is prescribed. Combining this condition and the axisymmetry presumed in Eq. (2) allows $\mathbf{n}$ to take only two symmetric orientations on the anchoring cone, which differ by the sign of φ_0 in Eq. (3). Here we take φ_0 to be positive. We shall soon see that reversing the sign of φ_0 has essentially no effect. We imagine that in filling the capillary tube one of these orientations is preferred to the other, possibly depending on the direction of filling.

Consider now the problem of finding a field $\mathbf{n}$ as in Eq. (2) which obeys Eq. (3) and minimizes the elastic free energy $\mathcal{E}$ stored in the cylinder. In the one-constant approximation, this energy has a density per unit volume given by

$$\sigma:=\frac{K}{2}|\nabla\,\mathbf{n}|^2, \tag{4}$$

where K is a positive modulus. It is shown in [15] that, for $-\pi/2<\varphi_0<\pi/2$, there are exactly two stationary points for $\mathcal{E}$, which we call $\mathbf{n}_-$ and $\mathbf{n}_+$, obtained by inserting into Eq. (2) the following expressions for φ:

$$\varphi_-(r,z)=\arcsin\left(\frac{R^2\cos^2\varphi_0-(1-\sin\varphi_0)^2r^2}{R^2\cos^2\varphi_0+(1-\sin\varphi_0)^2r^2}\right) \tag{5}$$

and

$$\varphi_+(r,z)=-\arcsin\left(\frac{R^2\cos^2\varphi_0-(1+\sin\varphi_0)^2r^2}{R^2\cos^2\varphi_0+(1+\sin\varphi_0)^2r^2}\right). \tag{6}$$

Figures 1(a) and 1(b) illustrate $\mathbf{n}_-$ and $\mathbf{n}_+$, respectively, for $\varphi_0>0$. Simple computations show that $\mathbf{n}_-$ is the absolute minimizer for the elastic free energy, while more labor is required (cf. [15]) to prove that $\mathbf{n}_+$ is a local minimizer. Notice that for the homeotropic anchoring, both $\mathbf{n}_-$ and $\mathbf{n}_+$ reduce to one and the same field, which is often referred to as the *escaped field* since it was discovered by Cladis and Kléman [6] and Meyer [7] in the early 1970s. As soon as φ_0 is different from zero, the equilibrium solution splits into two different fields, which store different elastic energies. They also are qualitatively different: in one field the director escapes in the same direction as the boundary data, while in the other field it escapes in the opposite direction, turning by an angle larger than $\pi/2$.

We construct a class of fields that bear either a $+1$ or a -1 defect, elaborating on the idea that such defects appear when a field that escapes upwards along the axis joins another which escapes downwards, or *vice versa*. This junction is performed through two axisymmetric free surfaces, which we call the *joints*, as illustrated in Fig. 1(c) for a $+1$ defect. Notice that for $\varphi_0<0$ the prototype for a $+1$ defect would be

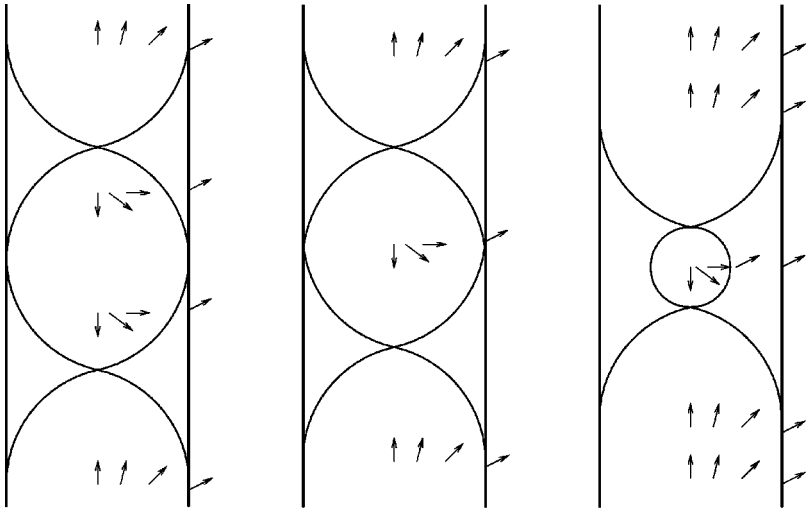

FIG. 2. Sketch of the director field during the interaction between two defects of opposite topological charge.

described by Fig. 1(c) reversed upside down. Moreover, a -1 defect can also be modeled by joining together the fields in Figs. 1(a) and 1(b), with the latter on top of the former [see Fig. 1(d)].

In Fig. 1(c) an escaped field is rescaled on each section orthogonal to the axis of the cylinder, so that $\varphi=\varphi_0$ on the joints; moreover, in the peripheral region between the joints and the lateral boundary of the tube, the director field is constant on each section with constant ϑ. The free surfaces meet at a point along the axis, which is a singular point for $\mathbf{n}$: it is either a $+1$ or a -1 defect depending on whether the field pointing upwards occurs above or below it. Hereafter, we focus attention on a $+1$ defect, since every result valid for it can easily be rephrased for a -1 defect.

Let h_1 and h_2 be the unknown heights of the joints and let $r=r_1(z)$ and $r=r_2(z)$ be the unknown functions that describe their longitudinal section. We call $\mathbf{n}_1$ and $\mathbf{n}_2$ the director fields just described in words, which in Fig. 1(c) are shown above and below the defect. They are determined, respectively, by giving the function φ in Eq. (2) the following forms:

$$\varphi_1(r,z)=\begin{cases}\arcsin\left(\dfrac{r_1^2\cos^2\varphi_0-(1-\sin\varphi_0)^2r^2}{r_1^2\cos^2\varphi_0+(1-\sin\varphi_0)^2r^2}\right), & 0\leqslant r\leqslant r_1(z),\\ \varphi_0, & r_1(z)\leqslant r\leqslant R,\end{cases} \tag{7}$$

$$\varphi_2(r,z)=\begin{cases}\arcsin\left(\dfrac{(1+\sin\varphi_0)^2r^2-r_2^2\cos^2\varphi_0}{r_2^2\cos^2\varphi_0+(1+\sin\varphi_0)^2r^2}\right), & 0\leqslant r\leqslant r_2(z),\\ \varphi_0, & r_2(z)\leqslant r\leqslant R.\end{cases} \tag{8}$$

We do not dwell further on the mathematical details of this model, which could easily be retraced in [15], where another application is considered. We only note that the problem of finding the joints with the minimum energy has a unique solution, provided that their heights obey the following inequalities:

$$h_1\leqslant\frac{\sqrt{A(\varphi_0)\,\pi}}{\cos\varphi_0}R \quad\text{and}\quad h_2\leqslant\frac{\sqrt{A(-\varphi_0)\,\pi}}{\cos\varphi_0}R, \tag{9}$$

where

$$A(\varphi_0)\coloneqq\frac{1+\sin\varphi_0}{1-\sin\varphi_0}\{2\ln 2-1-2\ln(1+\sin\varphi_0)+\sin\varphi_0\}. \tag{10}$$

III. INTERACTION FORCE

Our purpose in this section is to describe how two defects with opposite topological charges interact. Consider a cylinder with a prescribed anchoring angle φ_0 on its lateral boundary and with height $2H$ sufficiently large to accommodate two defects together with their joints. Let two defects with topological charges $+1$ and -1 be on the axis of the

cylinder, and let the field $\mathbf{n}_+$ described in Sec. II be in the region between them. Since by the second inequality in (9) the maximum height of the inner joints in Fig. 2 is bounded, the distortions associated with the defects would not interfere with one another as long as the distance d between these remains larger than

$$d_c := 2\frac{\sqrt{A(-\varphi_0)\pi}}{\cos\varphi_0}R. \tag{11}$$

Thus, a strip with the equilibrium field $\mathbf{n}_+$ lies between the inner joints. Bringing the defects closer to one another then implies rearranging the director field $\mathbf{n}$ so that this strip is shortened: the two joints come closer, rigidly sliding along the tube, while the regions away from the defects, where $\mathbf{n}=\mathbf{n}_-$, become larger. As shown in [14], no interaction between the defects is responsible for this motion: it results from two independent motions, each due to a constant force.

When $d<d_c$ the height of both inner joints in Fig. 2 is $d/2$. The equilibrium distortion for $\mathbf{n}$ is shown in Fig. 2(c). To compute the elastic free energy stored in the whole cylinder, we first evaluate the energy of the inner joints, which enclose a rescaled field $\mathbf{n}_+$, then the energy of the outer joints, which embrace a rescaled field $\mathbf{n}_-$, and finally the energy of the regions near the ends of the cylinder, where $\mathbf{n}_-$ need not be rescaled. Details of such computations are given in [15]; here we only report the final expression for the total elastic free energy $\mathcal{E}$ as a function of d:

$$\mathcal{E}(d)=\pi K\left\{4\sin\varphi_0+\cos^2\varphi_0\left(1-\ln\frac{d}{d_c}\right)\right\}d+\mathcal{E}(0)$$
$$\text{for}\quad d\leqslant d_c, \tag{12}$$

where

$$\mathcal{E}(0)=2\pi K\{\cos\varphi_0\sqrt{A(\varphi_0)\pi}R+HB(\varphi_0)\}$$

with

$$B(\varphi_0):=2(1-\sin\varphi_0).$$

The force $f(d)$ acting on each defect is defined by

$$f(d):=-\mathcal{E}'(d), \tag{13}$$

where a prime now denotes differentiation with respect to d. It readily follows for Eq. (12) that

$$f(d)=-\pi K\left\{4\sin\varphi_0-\cos^2\varphi_0\ln\frac{d}{d_c}\right\}\quad\text{for}\quad d\leqslant d_c. \tag{14}$$

A glance at Eq. (11) would suffice to remind the reader that here d_c depends on φ_0: it is a decreasing function defined for $0\leqslant\varphi_0\leqslant\pi/2$, which at $\varphi_0=0$ equals the critical distance for the homeotropic anchoring, slightly above $2.2R$, and tends approximately to $1.7R$ for $\varphi_0\to\pi/2$. This limiting case deserves notice: the director field $\mathbf{n}$ tends indeed to become uniform around the defects, apart from a whole singular straight string linking them, while the joints fade away and the *tension* in the string approaches $2\pi K$. We refer the reader to [15] for further details on this.

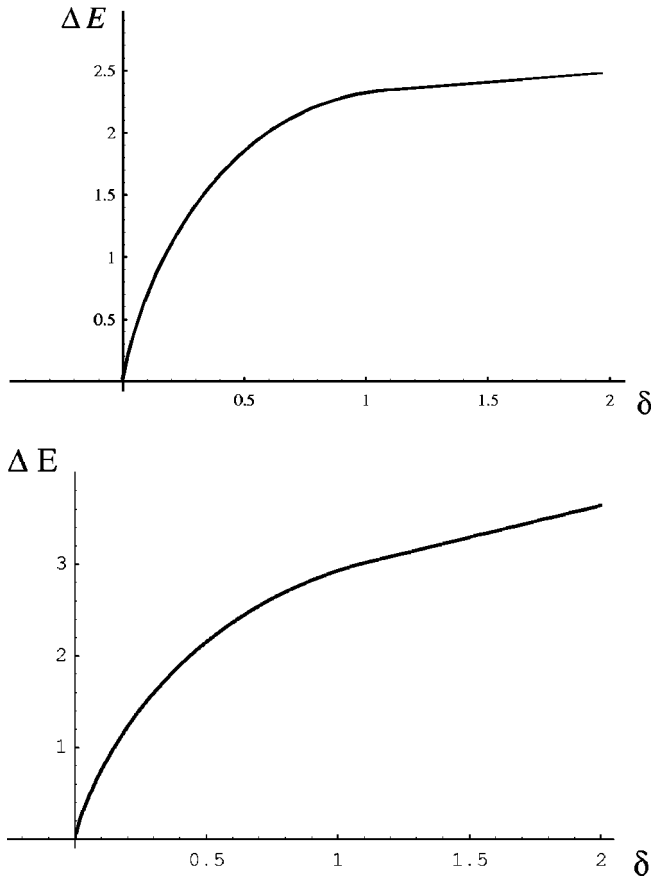

FIG. 3. The graph of the dimensionless function ΔE against the dimensionless distance between the defect δ for $\varphi_0=1°$, 2nd $\varphi_0=5°$, respectively.

The graph of the dimensionless function $\Delta E:=(E(d)-\mathcal{E}(0))/\pi KR$ against the dimensionless distance between the defects $\delta:=d/2R$ is plotted in Figs. 3(a) and 3(b) for $\varphi_0=1°$ and $\varphi_0=5°$, respectively.

IV. DYNAMICS

Here we derive the equation of motion that governs the coalescence between two defects with opposite topological charges. The classical theory for nematic flow has recently been rebuilt by Leslie [16] on a dissipation principle, which takes the following form when the hydrodynamic flow is negligible:

$$\dot{\mathcal{E}}+\mathcal{W}=0; \tag{15}$$

here a superimposed dot denotes the time derivative and $\mathcal{W}$ represents the energy dissipated by the viscous torques acting on the director $\mathbf{n}$. Since the molecular inertia is negligible, no account is taken in Eq. (15) for the kinetic energy involved in the motion of the director field.

In applying Eq. (15) to the present case, we assume that the configurations traversed by the director field during the coalescence of the defects are the equilibrium configurations described above. Thus, once the dissipation function $\mathcal{W}$ is known as a function of the distance d between the defects and its time derivative, Eq. (15) becomes a first-order differential equation for d. We skip again the technical aspects of

this computation, referring the reader to [15], where $\mathcal{W}$ was computed for a setting that formally differs from this only by the sign of φ_0: here the appropriate formula for $\mathcal{W}$ is

$$\mathcal{W}=\frac{1}{2}\pi^{3/2}\gamma_1 R\cos\varphi_0\left\{\lambda\sqrt{A(-\varphi_0)}\frac{d}{d_c}+\sqrt{A(\varphi_0)}\right\}\dot{d}^2 \quad \text{for } d<d_c, \tag{16}$$

where $\gamma_1>0$ is the rotational viscosity (cf., e.g., Chap. 5 of [17]) and $\lambda\simeq 1.445$ is a dimensionless parameter which has been computed numerically, precisely as in [5].

We are now in a position to write the equation of motion for the defects. Inserting Eqs. (12) and (16) into Eq. (15), we arrive at

$$\frac{\dot{d}}{2R}=-\frac{1}{\tau}\frac{4\sin\varphi_0-\cos^2\varphi_0\ln\frac{d}{d_c}}{\sqrt{\pi}\cos\varphi_0\left\{\sqrt{A(-\varphi_0)}\lambda\frac{d}{d_c}+\sqrt{A(\varphi_0)}\right\}} \quad \text{for } d<d_c, \tag{17}$$

where $\tau:=\gamma_1 R^2/K$ is a characteristic time, which also depends on the capillary radius. We can obtain from Eq. (17) the time t as a function of d:

$$t(d)=t_a-\frac{\tau}{2R}\times\int_0^d\frac{\sqrt{\pi}\cos^2\varphi_0\left\{\sqrt{A(-\varphi_0)}\lambda\frac{x}{d_c}+\sqrt{A(\varphi_0)}\right\}}{4\sin\varphi_0-\cos^2\varphi_0\ln\frac{x}{d_c}}dx, \quad d<d_c, \tag{18}$$

where $t_a:=t(0)$ represents the *annihilation time*, which depends on the initial distance d_i:

$$t_a=\frac{\tau}{2R}\int_0^{d_c}\frac{\sqrt{\pi}\cos^2\varphi_0\left\{\sqrt{A(-\varphi_0)}\lambda\frac{x}{d_c}+\sqrt{A(\varphi_0)}\right\}}{4\sin\varphi_0-\cos^2\varphi_0\ln\frac{x}{d_c}}dx+\frac{\sqrt{\pi}[\sqrt{A(-\varphi_0)}+\sqrt{A(\varphi_0)}]}{4\tan\varphi_0}(d_i-d_c). \tag{19}$$

We obtain from Eq. (18) the graph of the dimensionless distance δ against the dimensionless time to annihilation $(t_a-t)/\tau$. In Fig. 4 this graph is drawn for both $\varphi_0=1°$ and $\varphi_0=5°$ together with the one borrowed from [5], which corresponds to the homeotropic anchoring ($\varphi_0=0°$). A dashed line illustrates the linear decay of the distance in time, which lasts until the interaction starts, that is, as long as d exceeds the critical distance d_c. We also see from Fig. 4 that d_c depends on φ_0 and that the phenomenon becomes faster as this angle increases.

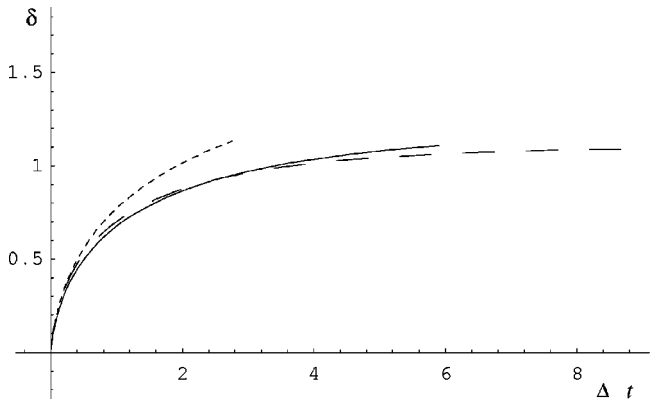

FIG. 4. Graph of the dimensionless distance δ against the dimensionless time to annihilation Δt: the dashed line is for $\varphi_0=0°$, the dotted for $\varphi_0=5°$, and the continuous line for $\varphi_0=10°$.

V. DISCUSSION

One might well argue that the phenomenon we have attempted to model is more complex than it appears here. In particular, the backflow, which has so far been completely neglected, is expected to play a role in the motion of colliding defects, especially when they come sufficiently close to one another. It should create a vorticity confined in a region closing up with the defects: its contribution to the dynamics should be an effective, possibly nonuniform, reduction of γ_1, as suggested by the study of simpler cases (see [12] and [13]).

A naive way of accounting for this contribution would be the following. First, we imagine that the closer the defects, the more the backflow favors their attraction. Second, to avoid computing the dissipation in the hydrodynamic flow, we simply assume that this amounts to an effective rotational viscosity γ_1 which decreases with the distance d between the defects. Here, for example, we take γ_1 proportional to d^2: Fig. 5 shows for $\varphi_0=1°$ how the annihilation law would depart from that with constant viscosity. Maybe this is too crude an approximation, but it suggests how sensitive the annihilation of defects could be to the backflow.

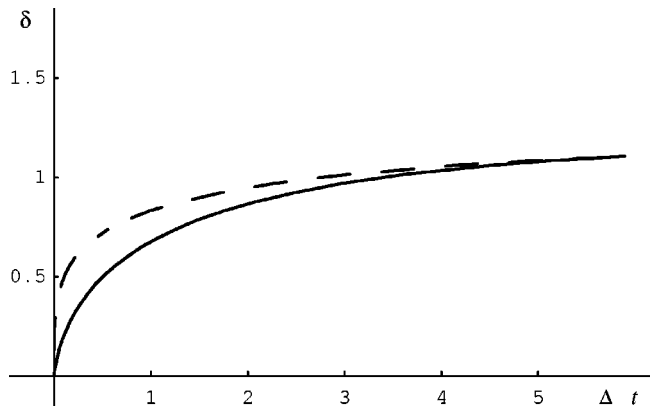

FIG. 5. The continuous line shows the dimensionless distance between the defects against the dimension annihilation time for $\varphi_0=1°$ and a constant γ_1, while the dashed line is plotted for γ_1 proportional to $(\delta/\delta_i)^2$.

[1] N. D. Mermin, Rev. Mod. Phys. **51**, 591 (1979).
[2] G. E. Volovik and O. D. Lavrentovich, Zh. Éksp. Teor. Fiz. **85**, 1997 (1983) [Sov. Phys. JETP **58**, 1159 (1983)].
[3] J. L. Ericksen, Trans. Soc. Rheol. **5**, 22 (1961).
[4] F. M. Leslie, Arch. Ration. Mech. Anal. **28**, 265 (1968).
[5] G. Guidone Peroli and E. G. Virga, Phys. Rev. E **54**, 5235 (1996).
[6] P. E. Cladis and M. Kléman, J. Phys. (Paris) **33**, 591 (1972).
[7] R. B. Meyer, Philos. Mag. **77**, 405 (1973).
[8] G. Guidone Peroli and E. G. Virga, Physica D **111**, 356 (1998).
[9] G. Guidone Peroli and E. G. Virga, Phys. Rev. E **56**, 1819 (1997).
[10] P. Biscari, G. Guidone Peroli, and E. G. Virga (unpublished).
[11] S. Kralj and S. Žumer (private communication).
[12] F. Brochard, Mol. Cryst. Liq. Cryst. **23**, 51 (1973).
[13] G. E. Durand and E. G. Virga, Phys. Rev. E (to be published).
[14] G. Guidone Peroli, G. Hillig, A. Saupe, and E. G. Virga, Phys. Rev. E **58**, 3259 (1998).
[15] G. Guidone Peroli and E. G. Virga, Commun. Math. Phys. (to be published).
[16] F. M. Leslie, Continuum Mech. Thermodyn. **4**, 167 (1992).
[17] P. G. de Gennes and J. Prost, *The Physics of Liquid Crystals*, 2nd ed. (Clarendon Press, Oxford, 1993).